SAND2000-1298C

GaInNAs Laser Gain

W. W. Chow, E. D. Jones, N. A. Modine, S. R. Kurtz and A. A. Allerman

Sandia National Laboratories
Albuquerque, NM 85718-0601, U. S. A.

Abstract

The optical gain spectra for GaInNAs/GaAs quantum wells are computed using a microscopic laser theory. From these spectra, the peak gain and carrier radiative decay rate as functions of carrier density are determined. These dependences allow the study of the lasing threshold current density of GaInNAs/GaAs quantum well structures.

1. Introduction

The GaInNAs alloy system has the advantages of emission at wavelengths important for fiber optic communications, and close lattice match to GaAs.[1] This theoretical paper addresses some of the issues concerning quantum well lasers based on this material system. In particular, we are interested in the optical properties, expected device performance, and optimal laser configuration.

We consider the quantum well structures, $Ga_{0.93}In_{0.07}N_{0.02}As_{0.98}$/GaAs and $Ga_{0.7}In_{0.3}N_{0.004}As_{0.996}$/GaAs. The latter is compressively strained and is used in early GaInNAs lasers.[1] The former is interesting because $Ga_{0.93}In_{0.07}N_{0.02}As_{0.98}$ has a bandgap energy around 1eV, and yet is lattice matched to GaAs. While compressive strain in general improves laser properties, the lattice-matched structure allows the growth of thick active layers (as in epilayers and superlattices) that improve spatial overlap with the optical field.

The aforementioned structures are also chosen to illustrate strain effects on optical properties. While some of the strain effects are similar to those in other semiconductor lasers, there are important differences as well. Section II describes some of these differences, and the calculation of the bandstructure properties needed for computing the laser gain. Section III discusses the gain calculationsw and shows examples of gain spectra. In Sec. IV, we extract from the gain spectra the carrier density dependence of peak gain. More important in terms of laser performance are the peak gain versus current density relations described in Sec. V. We show in this section that significant differences can result in the carrier density and current density dependences of peak gain. These differences are very apparent when we make comparisons between the two GaInNAs/GaAs structures, and between these structures and those involving GaInAs/InP, a commonly used material system for long-wavelength semiconductor lasers.

2. Bandstructure

In this section, we discuss the compilation of the GaInNAs material parameters needed for the gain calculations. For small nitrogen concentrations, most of the $Ga_{1-x}In_xN_yAs_{1-y}$ material parameters may be approximated by the corresponding ones for $Ga_{1-x}In_xAs$.[2] Exceptions are the bandgap energy and electron effective mass, where we use phenomenological expressions reported in earlier. For the bandgap energy,[1]

$$\varepsilon_{g0}(Ga_{1-x}In_xN_yAs_{1-y}) = \varepsilon_{g0}(Ga_{1-x}In_xAs) - 69eV \times \Delta e(x,y),$$

where

$$\Delta e(x,y) = e(x,y) - e(x,0)$$

DISCLAIMER

DISCLAIMER

Portions of this document may be illegible in electronic image products. Images are produced from the best available original document.

is the difference between the strain computed for $Ga_{1-x}In_xN_yAs_{1-y}$ and $Ga_{1-x}In_xAs$,

$$e(x,y) = \frac{a(0,0) - a(x,y)}{a(x,y)},$$

and a(x,y) is the lattice constant for $Ga_{1-x}In_xN_yAs_{1-y}$. For the electron effective mass,[3]

$$m_e(Ga_{1-x}In_xN_yAs_{1-y}) = m_e(Ga_{1-x}In_xAs) + 18.1667m_0 \times \Delta e(x,y),$$

where m_0 is the free electron mass. The above equation gives significantly different electron effective masses for $Ga_{0.93}In_{0.07}N_{0.02}As_{0.98}$/GaAs and $Ga_{0.7}In_{0.3}N_{0.004}As_{0.996}$/GaAs, consistent with experiment.[4] The values of ε_{g0} and m_e calculated for these two alloys, together with the other parameters needed for the quantum well bandstructure calculations are listed in Table 1 of Ref [3].

Based on results from bandstructure calculations involving the bulk alloy,[4] we assume in the $Ga_{1-x}In_xN_yAs_{1-y}$ quantum well bandstructure calculations that the presence of nitrogen affects mainly the conduction band. Then, to a good approximation, we can compute the hole bandstructure by performing a **k•p** calculation for a $Ga_{1-x}In_xAs$-GaAs quantum well structure, where we assume that the strain is e(x,y), i.e., similar to that in $Ga_{1-x}In_xN_yAs_{1-y}$ /GaAs. For the lattice-matched structure, the hole bandstructure consists of two heavy hole subbands (hh1 and hh2) and one light hole subband (lh1). In contrast, only the heavy hole is Type 1 in the compressive-strained structure, leading to much higher hole band curvatures.

3. Gain Spectrum

To study the bandstructure influence on optical properties, we calculate the gain spectra for the $Ga_{0.93}In_{0.07}N_{0.02}As_{0.98}$/GaAs and $Ga_{0.7}In_{0.3}N_{0.004}As_{0.996}$/GaAs quantum well structures. The calculations are based on the semiconductor Bloch equations, with carrier-carrier collisions treated at the level of quantum kinetic equations.[5] Figure 1 shows the room temperature TE and TM gain spectra for the lattice-matched quantum well at different carrier densities. The two polarizations describe electric field polarization in (TE) and perpendicular to (TM) the plane of the quantum well. For the same carrier density, the spectra show approximately equal gain in the two polarizations, which is typical for unstrained quantum wells. Figure 2 shows noticeably different behaviors for the compressive-strained quantum well. In particular, the gain is higher for a given carrier density than is the case for the unstrained structure. Because the structure contains only heavy hole bound states, the TM absorption and gain are highly attenuated, and therefore not shown.

4. Peak Gain versus Carrier Density

Figure 3 shows that compared to the lattice-matched structure, the compressive-strained quantum well has significantly lower transparency carrier density and higher differential gain dG/dN. These differences are due to differences in band curvatures. The higher electron and hole curvatures in the compressive-strained structure lead to smaller joint densities of states, which in turn make the creation of a population inversion easier. For comparison, we also plotted the curve for a 5nm $Ga_{0.67}In_{0.33}As$-InP quantum well, which is representative of a more developed material system for long-wavelength semiconductor lasers. To obtain an emission energy that is approximately that of the other structures, we choose an In concentration of 0.33, which results in an e = 0.02 tensile strained quantum well. As the hole curvatures for the lattice-matched GaInNAs/GaAs and the tensile strained GaInAs/InP quantum wells are approximately similar, the difference in the transparency carrier densities for these two structures may be traced to the significantly larger electron effective mass in the former.

5. Peak Gain versus Current Density

Figure 4 shows the radiative carrier recombination rate w_{sp} vs. carrier density for the three gain structures. To calculate w_{sp}, we use a phenomenological relationship that relates the spontaneous emission and gain spectra.[6] Combining the results of Figs. 3 and 4 gives the dependence of peak gain on the spontaneous emission current density. The spontaneous emission current density is $J_{sp} = ew\, w_{sp}$, where e is the electron charge, and w is the quantum well width. The curves in Fig. 5 give the theoretical limit to the threshold current density for threshold gain $G_{th} = G_{pk}$. They show that in spite of the large difference in transparency carrier density between the two GaInNAs/GaAs quantum wells, they have approximately the same transparency current densities, suggesting partial cancellation of bandstructure differences in a gain vs current density curve. Above transparency, bandstructure effects still play important roles, e.g., in giving a greater dG_{pk}/dJ_{sp} to the compressive-strained structure.

Comparison of the GaInAs/InP and GaInNAs/~~GaN~~ GaAs curves in Figs. 3 and 5 identifies another mechanism that causes G_{pk} vs N to be different than G_{pk} vs J_{sp} . In Fig. 3, we note that the transparency carrier density is greater in the lattice-matched GaInNAs/GaN quantum well than in GaInAs-InP. Figure 5 shows the reverse, with GaInAs/InP having the higher transparency current density. The explanation for this behavior involves the dipole matrix element. The transparency carrier density depends primarily on bandfilling effects and thus is sensitive to band curvatures, but not to the dipole matrix element. On the other hand, the radiative carrier recombination rate is proportional to the square of the dipole matrix element, and the larger dipole matrix element in GaInAs/InP leads to greater spontaneous emission loss, and consequently to a higher transparency current density. The spontaneous emission losses at transparency for the three quantum well structures are shown by the dots in Fig. 4.

6. Conclusion

In summary, we use a many-body microscopic laser theory to investigate the gain and threshold current properties of GaInNAs/GaAs quantum wells. The calculations show gain properties that depend significantly on strain. Some of the strain effects are similar to those in other semiconductor lasers, especially effects arising from modifications to the hole bandstructure. However, the strain effects arising from conduction band and optical matrix element modifications are unique to the GaInNAs/GaAs system. These effects strongly influence the gain vs carrier density and gain vs current density relations.

Acknowledgments

This work was supported in part by the U. S. Department of Energy under contract No. DE-AC04-94AL85000.

References

1. M. Kondow, T. Kitatani, S. Nakatsuka, M. Larson, K.Nakahara, Y. Yazawa, M. Okai and K. Uomi, IEEE J. Selected Topics in Quantum Electron. **3**, 719 (1997).
2. L. Bellaiche, S.-H. Wei and A. Zunger, Phys. Rev B **54**, 17568 (1996).
3. W. W. Chow, E. D. Jones, N. A. Modine, A. A. Allerman, S. R. Kurtz , Appl. Phys. Lett. **75**, 2891 (1999).
4. E. D. Jones, N. A. Modine, A. A. Allerman, S. R. Kurtz, A. F. Wright, S. T. Tozer and X. Wei, Phys. Rev **B 60**, 4430 (1999).
5. W. W. Chow and S. W. Koch, *Semiconductor-Laser Fundamentals: Physics of the Gain Materials* (Springer, Berlin, 1999).
6. C. H. Henry, R. A. Logan and F. R. Merritt, J. Appl Phys. **51**, 3042 (1980).

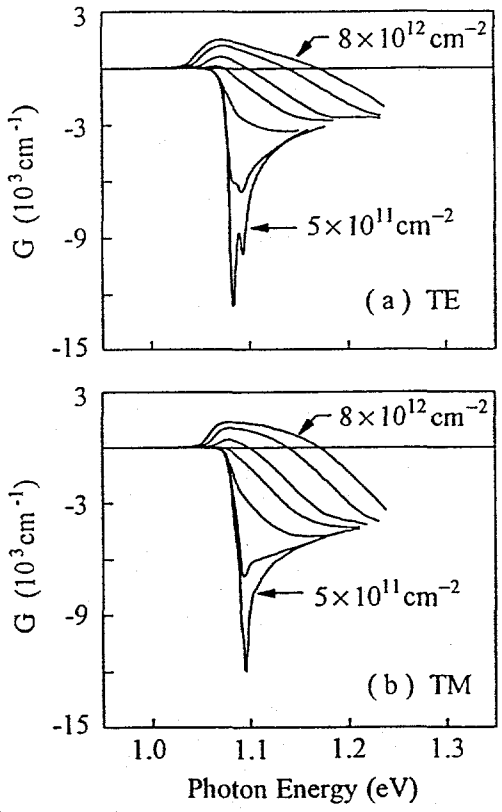

Fig. 1. Room temperature (a) TE and (b) TM gain spectra for lattice-matched 7nm $Ga_{0.93}In_{0.07}N_{0.02}As_{0.98}$/GaAs and carrier densities N = 0.5 ×, 1 ×, 2 ×, 3 ×, 4 ×, 6 × and 8 × 10^{12}cm^{-2}.

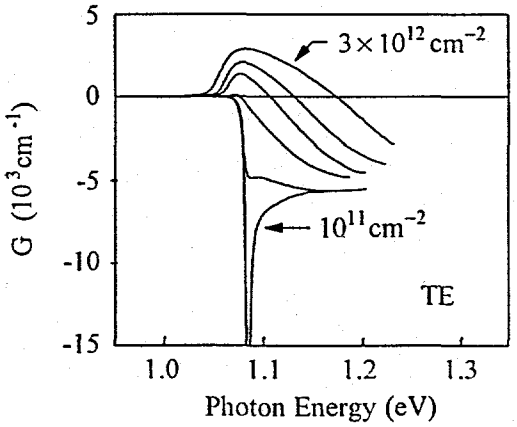

Fig. 2. Room temperature TE gain spectra for compressive-strained 7nm $Ga_{0.7}In_{0.3}N_{0.004}As_{0.996}$/GaAs quantum well and carrier densities N = 0.1 ×, 0.5 ×, 1.0 ×, 1.5 ×, 2.0 × and 3 × 10^{12}cm^{-2}.

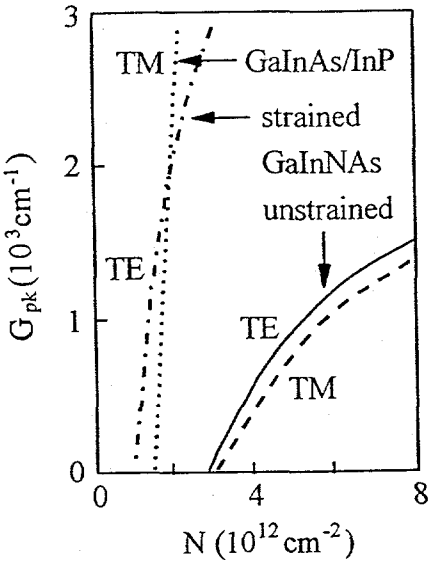

Fig. 3. Peak gain versus carrier density for TE (solid curve) and TM (dashed curve) polarization in lattice-matched GaInNAs/GaAs, TE polarization in compressive-strained GaInNAs/GaAs (dot-dashed curve), and TM polarization in tensile-strained GaInAs/InP (dotted curve).

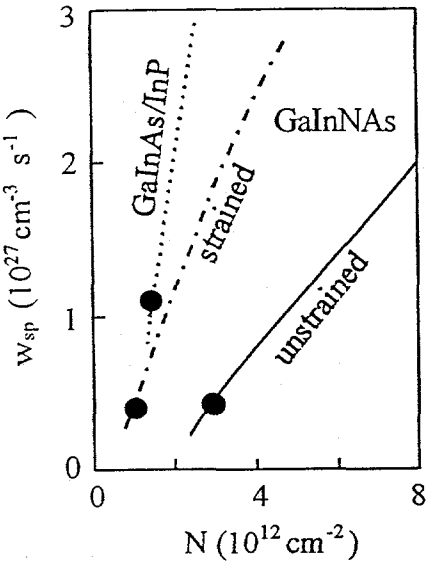

Fig. 4. Radiative carrier recombination rate vs carrier density for lattice-matched (solid curve) and compressive-strained (dot-dashed curve) GaInNAs-GaAs, and tensile-strained GaInAs/InP (dotted curve).

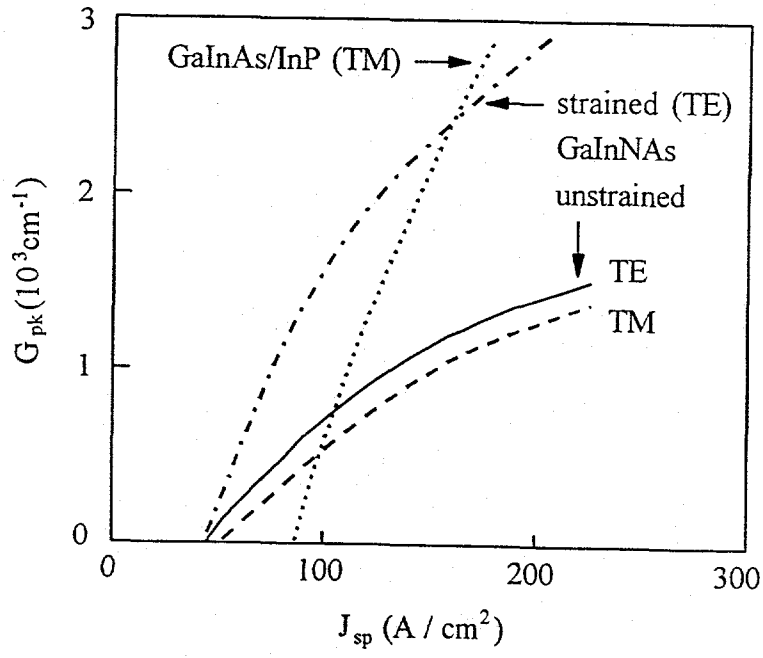

Fig. 5 Peak gain versus spontaneous emission current density for the three structures in Figs. 3 and 4. The notation is similar to the that in Fig. 3.